

A Quantitative Model of the Cardiac Ventricular Cell Incorporating the Transverse-Axial Tubular System

M. PÁSEK¹, G. CHRISTÉ² AND J. ŠIMURDA³

¹ *Institute of Thermomechanics, Czech Academy of Sciences, Branch Brno, Czech republic*

² *INSERM EMI 0219, DRDC/DVE, CEA Grenoble, France*

^{3,1} *Department of Physiology, Masaryk University, Brno, Czech Republic*

Abstract. The role of the transverse-axial tubular system (TATS) in electrical activity of cardiac cells has not been investigated quantitatively. In this study a mathematical model including the TATS and differential distribution of ionic transfer mechanisms in peripheral and tubular membranes was described. A model of ventricular cardiac cell described by Jafri et al. (1998) was adopted and slightly modified to describe ionic currents and Ca^{2+} handling. Changes of concentrations in the lumen of the TATS were computed from the total of transmembrane ionic fluxes and ionic exchanges with the pericellular medium. Long-term stability of the model was attained at rest and under regular stimulation. Depletion of Ca^{2+} by 12.8% and accumulation of K^+ by 4.7% occurred in the TATS-lumen at physiological conditions and at a stimulation frequency of 1 Hz. The changes were transient and subsided on repolarization within 800 ms (Ca^{2+}) and 300 ms (K^+). Nevertheless, the course of action potentials remained virtually unaltered. Simulations of voltage clamp experiments demonstrated that variations in tubular ionic concentrations were detectable as modulation of the recorded membrane currents.

Key words: Cardiac cell — Tubular system — Quantitative modelling

Introduction

Mathematical models of excitable cells have undergone a remarkable evolution since the pioneering work of Hodgkin and Huxley (1952). The modelling paradigm established by Hodgkin and Huxley uses the total current flowing through ion channels in the membrane to determine the transmembrane voltage. It became a cornerstone of numerous generalizations and modifications describing the electrical properties of a variety of excitable tissues, including cardiac cells (Noble 1962; McAllister et al.

Correspondence to: Dr. Michal Pásek, Institute of Thermomechanics, Czech Academy of Sciences, Branch Brno, Technická 2, 616 69 Brno, Czech Republic
E-mail: pasek@umtn.fme.vutbr.cz

1975; Beeler and Reuter 1977; Luo and Rudy 1991). A later stage in the evolution of the mathematical modelling of cardiac cells has been the development of models that account for dynamic changes in intracellular ionic concentrations (DiFrancesco and Noble 1985; Hilgemann and Noble 1987; Nordin 1993; Luo and Rudy 1994; Nygren et al. 1998). In addition to the electrical properties of the cellular membrane, the dynamic models describe the function of important intracellular compartments (fuzzy space, sarcoplasmic reticulum (SR)) and ionic buffers. Although the current structure of dynamic models has been widely accepted for studying the electromechanical activity of cardiac cells, several new experimental findings strongly suggest the necessity of its further development.

One of the phenomena that cannot be simulated and quantified by the mathematical models developed so far is the effect of transverse-axial tubular system (TATS) on the electrical activity of ventricular cardiomyocytes. Most of the ionic transfer mechanisms of ventricular cells are found both at the peripheral and at the tubular membranes (Doyle et al. 1986; Frank et al. 1992; Chen et al. 1995; Mays et al. 1995; McDonough et al. 1996; Shepherd and McDonough 1998; Takeuchi et al. 2000). Some of them are even preferentially located at the tubular membrane (Frank et al. 1992; Chen et al. 1995; Mays et al. 1995; Christé 1999; Takeuchi et al. 2000). This makes the accumulation-depletion of ions likely to take place in the lumen of the TATS. This phenomenon is considered to play a role in the initiation of cellular arrhythmias (Yasui et al. 1993; Amsellem et al. 1995; Christé 1999). With regard to the lack of direct experimental data, a quantitative model may become a significant tool to estimate the impact of the TATS on the electrical activity of cardiac cells.

Materials and Methods

Description of the model

Generally, the model is based on a quantitative description of electrical activity of the ventricular myocyte proposed by Luo and Rudy (1994) and modified by Jafri et al. (1998) for a new description of Ca^{2+} handling. Included are ionic transporting systems in surface and tubular membranes as well as description of the SR (uptake and release compartment) and Ca^{2+} buffers. The model also incorporates a subsarcolemmal compartment – a ‘fuzzy space’ that was proved to play a significant role in the process underlying Ca^{2+} release from SR (Sun et al. 1995) and calcium current inactivation (Zahradník et al. 1996). A schematic diagram of the model is shown in Fig. 1. The formulation of the TATS as well as the modifications we have introduced to the quantitative description of Jafri et al. (1998) are summarised in the following sections.

Geometric parameters

The dimensions of the ventricular myocytes (cylindrical geometry) were assumed to be: 100 μm length and 10 μm radius (the proportions of intracellular compartments remained unaltered).

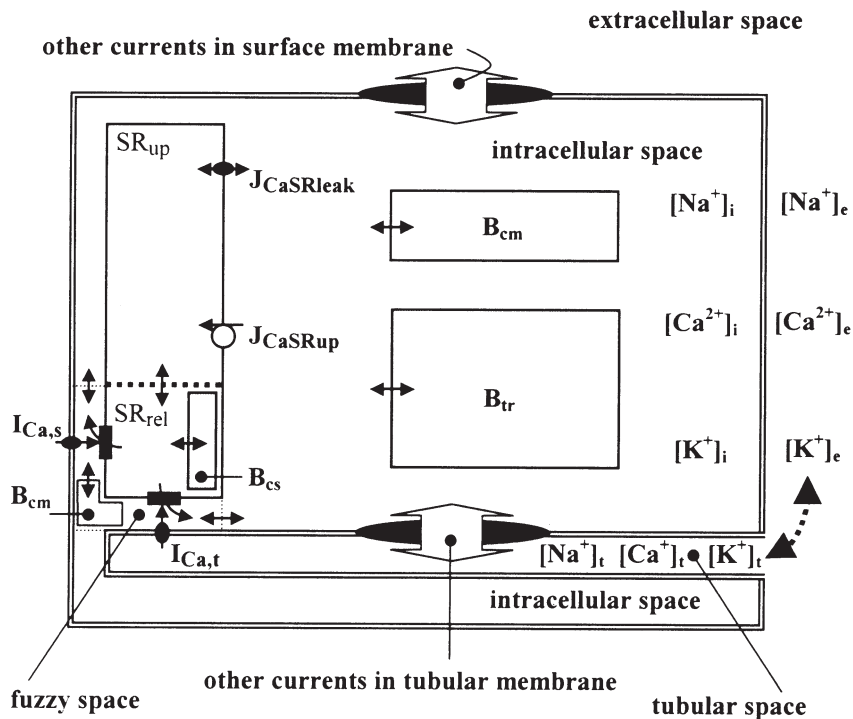


Figure 1. Schematic diagram of the ventricular cell model. The description of electrical activity of surface (s) and tubular (t) membrane comprises ionic currents (I_{Na} , I_{Ca} , I_K , I_{K1} , I_{Kp} , $I_{K(Na)}$, $I_{K(ATP)}$, $I_{ns(Ca)}$, $I_{Na,b}$, $I_{Ca,b}$, I_{NaCa} , I_{NaK} , I_{pCa}) introduced by Luo and Rudy (1994) and by Faber and Rudy (2000). In addition, the 4-aminopyridine-sensitive transient outward current I_{to} was incorporated. The intracellular space contains the fuzzy space, the Ca^{2+} -uptake and Ca^{2+} -release compartments of sarcoplasmic reticulum (SR_{up} , SR_{rel}) and the Ca^{2+} buffers calmodulin (B_{cm}), troponin (B_{tr}) and calsequestrin (B_{cs}). The small filled rectangles in SR_{rel} membrane represent ryanodine receptors. The small bi-directional arrows denote Ca^{2+} diffusion. Ionic diffusion between the tubular and the bulk space is represented by the dashed arrow.

The geometric parameters of the TATS were set according to the recent microscopic analysis on ventricular myocytes (Soeller and Cannell 1999). These parameters comprise the density of tubule mouths in the surface membrane (27.78×10^6 tubules/cm²), the average radius of the tubules ($r_t = 127 \times 10^{-7}$ cm) and their mean length ($l_t = 10$ μ m). The tubular membrane represented 69% of the total membrane area (2.23×10^{-4} cm²) and the fractional volume of the TATS was 3.12% of the cellular volume.

Ionic currents at surface and tubular membrane

The differences between the description of the surface and tubular membranes

pertain to the numeric values of the parameters. Both subsystems were described by the same set of differential equations (Jafri et al. 1998). The following modifications were introduced in the current model:

The description of I_{Na} -channel gating was restricted to three activation (m^3) and one inactivation (h) gates. The empirical formulas for the rate constants of activation (α_m , β_m) and inactivation (α_h , β_h) dependent on membrane voltage (V_m) were derived from the experimental data of Brown et al. (1981) and slightly modified according to our own experiments:

$$\begin{aligned}\alpha_m &= 117.26(V_m + 59.3)/(1 - \exp(-0.55(V_m + 59.3))) \\ \beta_m &= 3800 \exp(-0.0723(V_m + 61)) \\ \alpha_h &= 15.518/(1 + \exp(0.188(V_m + 68.2))) \\ \beta_h &= 18.77(V_m + 64.4)/(1 - \exp(-0.4(V_m + 64.4)))\end{aligned}\quad (1)$$

The reversal voltage of I_{Na} was decreased by introducing a fractional permeability of the channel for potassium ions (12% of sodium permeability) according to Nordin (1993).

The 4-AP-sensitive transient outward current I_{to} was incorporated into the model and described as

$$I_{to} = g_{to} r_1 (V_m - V_K) \quad (2)$$

where V_K is the Nernst reversal voltage of K^+ and g_{to} is a constant conductance (see Table 1). The fraction of open channels

$$r_1 = 1 - r_2 - r_3 - r_4 \quad (3)$$

results from the solution of a set of three differential equations

$$\begin{aligned}dr_2/dt &= \beta_r r_1 + \alpha_q r_3 - (\alpha_r + \beta_q) r_2 \\ dr_3/dt &= \beta_q r_2 + 0.05 \beta_r r_4 - (\alpha_q + 0.05 \alpha_r) r_3 \\ dr_4/dt &= \beta_q r_1 + 0.05 \alpha_r r_3 - (\alpha_q + 0.05 \beta_r) r_4\end{aligned}\quad (4)$$

Based on the experimental data (Šimurda et al. 1988; Tseng and Hoffman 1989), the rate constants α_q , β_q , α_r and β_r were expressed as

$$\begin{aligned}\alpha_q &= 395/(1 + \exp(-0.081(V_m + 0.9))) \\ \beta_q &= 356/(1 + \exp(0.0463(V_m + 12.4))) \\ \alpha_r &= 76 \exp(-(V_m + 80)/26.6)/(1 + \exp(0.4(V_m + 48))) \\ \beta_r &= 75 \exp((V_m - 50)/95.9)/(1 + \exp(-0.4(V_m + 49.4)))\end{aligned}\quad (5)$$

The model was also extended by a quantitative description of the Na-sensitive potassium current ($I_{K(Na)}$) and of the ATP-sensitive potassium current ($I_{K(ATP)}$) according to Faber and Rudy (2000).

The stimulus current (12 nA, 1 ms) was incorporated into the equation controlling the intracellular potassium concentration to comply with the charge conservation principle (Hund et al. 2001).

The maximal specific conductivity, permeability or current density of individual ionic transfer mechanisms in the surface and tubular membranes were set as summarised in Table 1 to comply with recent experimental data.

Table 1. Electrical properties of the surface and tubular membrane transport systems used in the model. The symbols g , P , and I_{\max} denote the maximal specific conductivity, permeability and current density of related transfer mechanisms, respectively. In the absence of data, the densities of ionic transfer mechanisms were assumed equal in both membrane systems. References: Petrecca et al. 1997 [1]; Yao et al. 1997 [2]; Mays et al. 1995 [3]; Christé 1999 [4]; Takeuchi et al. 2000 [5]; Shepherd and McDonough 1998 [6]; Frank et al. 1992 [7]; Chen et al. 1995 [8]; McDonough et al. 1996 [9]; Iwata et al. 1994 [10]

	unit	surface	tubules	references
g_{Na}	[mS/cm ²]	30	30	[1, 2]
g_{K}	[mS/cm ²]	0.18	0.02	[3]
g_{K1}	[mS/cm ²]	0.4838	0.8696	[4]
g_{to}	[mS/cm ²]	0.0645	0.116	[5]
g_{Kp}	[mS/cm ²]	0.002	0.002	
$g_{\text{K(Na)}}$	[mS/cm ²]	0.1285	0.1285	
$g_{\text{K(ATP)}}$	[mS/cm ²]	2.5157	4.5221	[4]
$g_{\text{Na,b}}$	[mS/cm ²]	0.0014	0.0014	
$g_{\text{Ca,b}}$	[mS/cm ²]	0.0021	0.0021	
P_{Ca}	[cm/s]	0.0054	0.0054	[6, 2]
$P_{\text{ns(Ca)}}$	[cm/s]	1.75×10^{-7}	1.75×10^{-7}	
$I_{\text{NaCa,max}}$	[$\mu\text{A}/\text{cm}^2$]	1290	2319	[7, 8]
$I_{\text{NaK,max}}$	[$\mu\text{A}/\text{cm}^2$]	1.5	1.5	[9]
$I_{\text{pCa,max}}$	[$\mu\text{A}/\text{cm}^2$]	2.9673	0.3334	[10]

Electrical interaction between surface and tubular membrane

As illustrated in Fig. 2, the TATS was described as a single compartment separated from the surface membrane by the mean resistance of the tubular system (R_{st}) connected to the bulk pericellular solution. The contribution of one tubule to R_{st} was expressed as the resistance of a cylindrical conductor whose length, radius and specific resistivity corresponded to one half of the tubular effective length ($l_t/2$), its average radius (r_t), and the specific resistivity of the extracellular solution (ρ_{ext}), respectively. (For the Tyrode solution, $\rho_{\text{ext}} \approx 83.33 \Omega \cdot \text{cm}$.) Taking into account that from the electric point of view the TATS represents a parallel combination of all (n_t) tubules in the model cell, the mean resistance of the tubular system can be calculated from the relation

$$R_{\text{st}} = \rho_{\text{ext}} l_t / (2\pi r_t^2 n_t) \quad (6)$$

As follows from the electrical equivalent scheme in Fig. 2, the stimulating current I_{m} equals the sum of the sarcolemmal current I_{ms} and the current through the TATS I_{mt} :

$$I_{\text{m}} = I_{\text{ms}} + I_{\text{mt}} \quad (7)$$

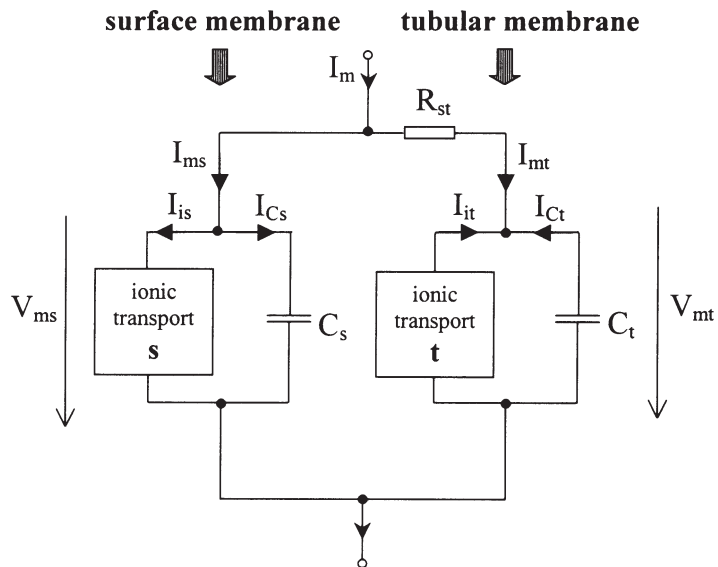


Figure 2. Electrical interaction between the surface and tubular membrane. V_{ms} , I_{is} , I_{Cs} , C_s and V_{mt} , I_{it} , I_{Ct} , C_t are, respectively, membrane voltage, total ionic current, capacitive current and membrane capacity of the surface and tubular membranes. R_{st} is the mean luminal resistance of the TATS.

In current clamp conditions $I_m = 0$ throughout except for the duration of the short (1 ms) suprathreshold stimuli. It follows that a common current

$$I_{circ} = I_{ms} = -I_{mt} = (V_{ms} - V_{mt})/R_{st} \quad (8)$$

circulates through both membrane systems.

Ionic diffusion between tubular and extracellular space

The time constants of ionic diffusion between the TATS and the extracellular space were set in the range of published data (Yao et al. 1997; Shepherd and McDonough 1998). They amounted to 300 ms for calcium ions and 120 ms for potassium and sodium ions.

Numerical solution of the model equations

The model was implemented in the program system MATLAB 6.0 (developed by the MathWorks, Inc.) and the numerical computation of the system of 57 non-linear differential equations was performed using the solver for stiff systems ODE-15s.

The basic units in which the equations were solved were: mV for membrane voltage, μA for membrane currents, mmol/l for ionic concentrations, s for time, and ml for volumes.

Results

Fig. 3 and Fig. 4 illustrate the basic behaviour of the model. Fig. 3 depicts steady state electrical responses of the surface and tubular membrane to stimulation pulses

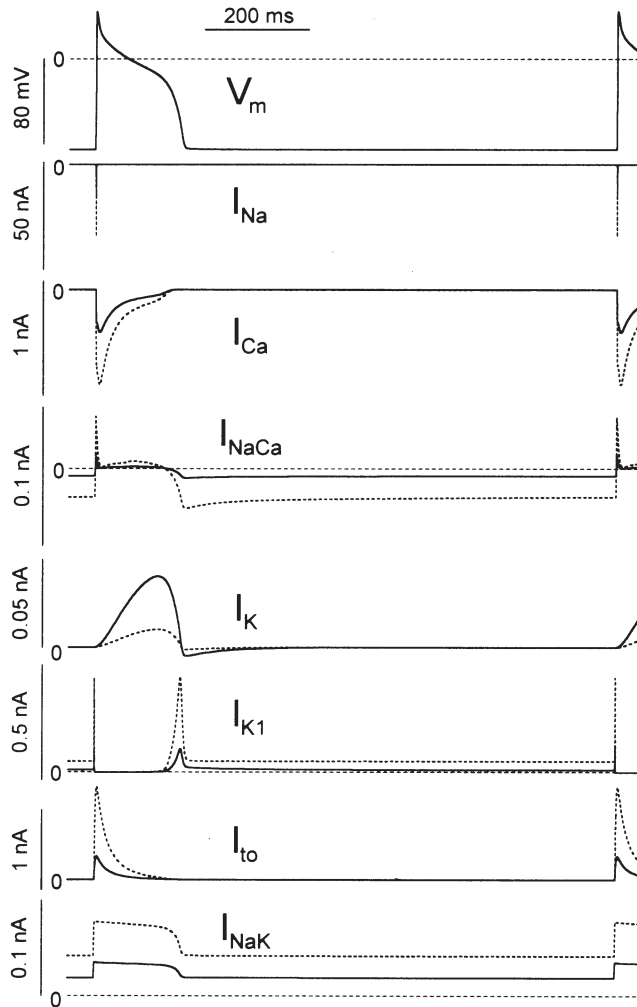


Figure 3. Action potentials (V_m) and main ionic currents in the surface (solid lines) and tubular (dotted lines) membrane in response to stimulation pulses (12 nA, 1 ms) applied at steady state (1 Hz). The currents visualised here are: I_{Na} , fast sodium current; I_{Ca} , calcium current through L-type channels; I_K , delayed rectifier potassium current; I_{K1} , inwardly rectifying potassium current; I_{to} , transient outward current; I_{NaCa} , sodium-calcium exchange current; and I_{NaK} , sodium-potassium pump current.

(12 nA, 1 ms) applied at 1 Hz. Included are action potentials and main ionic currents underlying depolarization (I_{Na} , I_{Ca}) and repolarization (I_K , I_{K1} , I_{to}) of the surface and tubular membrane. The carrier-mediated currents I_{NaK} and I_{NaCa} maintain ionic homeostasis. The remaining currents, of lesser importance with respect to modulation of AP, are not illustrated. The differences between APs of both membrane systems appeared to be negligible. The striking differences between the magnitudes of the surface (solid lines) and the tubular (dotted lines) membrane currents result from the different area of the tubular membrane and surface membrane, as well as from unequal densities of some channels, exchangers or pumps (see Table 1).

Fig. 4 depicts the changes of ionic concentrations in the SR, cytoplasm and TATS accompanying the electrical responses of Fig. 3. The transient increase in

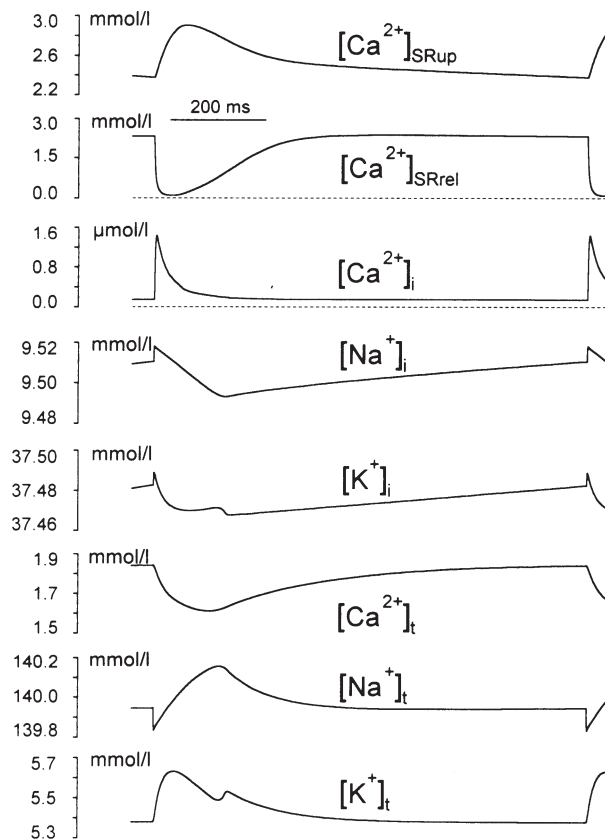


Figure 4. Concentration changes of Ca^{2+} in the uptake and release compartments of sarcoplasmic reticulum ($[Ca^{2+}]_{SRup}$, $[Ca^{2+}]_{SRrel}$), and of Ca^{2+} , K^+ , Na^+ in the myoplasm ($[Ca^{2+}]_i$, $[Na^+]_i$, $[K^+]_i$) and in the TATS ($[Ca^{2+}]_t$, $[Na^+]_t$, $[K^+]_t$). Steady-state at 1 Hz stimulation.

$[Ca^{2+}]_i$ from the diastolic level (140 nmol/l) to 1.4 $\mu\text{mol/l}$ occurs early after the onset of AP and reflects the rapid release of Ca^{2+} from the release compartment SR_{rel} (Fig. 1). It is mirrored as a fall of $[Ca^{2+}]_{SRrel}$ from 2.33 mmol/l to 0.1 mmol/l. The subsequent decline of $[Ca^{2+}]_i$ caused by the concurrent Ca^{2+} uptake into the uptake

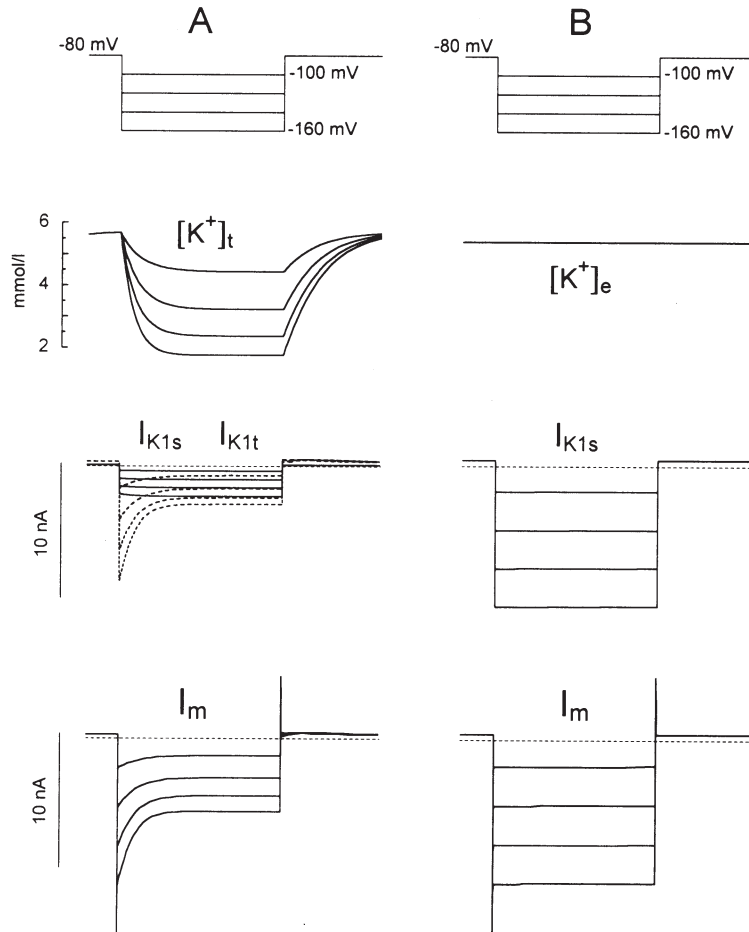


Figure 5. Modulation of the membrane current induced by changes of K^+ concentration in the TATS-lumen. In simulated voltage clamp regime, gradually increasing hyperpolarizing impulses were imposed from a holding voltage of -80 mV to voltages between -100 and -160 mV (20 mV steps). The traces from the top: command voltage, external K^+ concentrations $[K^+]_t$ and $[K^+]_e$, inward rectifier current I_{K1} , total membrane current I_m . **A.** Complete model. I_{K1s} , full traces; I_{K1t} , dashed traces. The small deviations of I_{K1s} from the constant level at the beginning of responses to hyperpolarizing steps result from the voltage drop on the series resistance ($1\text{ M}\Omega$) included in the model. **B.** Model deprived of the TATS.

compartment SR_{up} and calcium extrusion by the Na/Ca exchanger is considerably modulated by intracellular Ca^{2+} buffers (troponin and calmodulin). The relative changes of $[Na^+]_i$ and $[K^+]_i$ at a steady state are low. All diastolic levels of the intracellular concentrations lie in the range of reported values at 1 Hz stimulation frequency (Baumgarten et al. 1981; Siri et al. 1991; Harrison et al. 1992).

The most significant feature of the present model is its ability to simulate the dynamic changes of ionic concentrations in the TATS ($[Ca^{2+}]_t$, $[K^+]_t$, $[Na^+]_t$). Their relative values are 12.8% for $[Ca^{2+}]_t$, 4.7% for $[K^+]_t$ and 0.3% for $[Na^+]_t$ during regular action potential generation at a frequency of 1 Hz.

As the model predicted only a small effect of the TATS on the shape of the normal AP, further simulations were focused on voltage clamp experiments. The large potassium inward current I_{K1} evoked by progressively increased hyperpolarizing steps caused a considerable depletion of K^+ in the lumen of the TATS (Fig. 5A). In return, the lowered $[K^+]_t$ induced a prominent decline of I_{K1} that was clearly visible on the total membrane currents. In contrast, I_{K1} simulated with a model that had been deprived of the TATS followed (at constant $[K^+]_e$) the course of the membrane voltage (Fig. 5B).

Discussion

The exact description of propagation of electrical signals in the TATS requires a set of partial differential equations. In this work, a simple lumped-parameter approximation described by ordinary differential equations was used. This simplification is justified by the results of several approximate calculations. The maximum length of the T-tubules (25 μm) (Soeller and Cannell 1999) is much lower than the space constant of the T-tubule ($\lambda_t \cong \sqrt{r_m/r_t} \approx 240 \mu m$; calculated for the resting state under the assumption of a specific membrane resistance of 6.7 $k\Omega \cdot cm^2$ (Daut 1982) and a specific resistivity of the extracellular solution of 83.33 $\Omega \cdot cm$). Furthermore, under normal conditions, the calculated action potentials as generated by the surface membrane are nearly identical with the action potentials in the tubular system (Fig. 3). This is a consequence of the very short time constant $\tau_t = R_{st}C_t = 6.54 \mu s$ relating to the TATS. On real cells, in spite of the presence of the TATS, the capacitive current recorded in voltage clamp experiments has been currently approximated fairly well by a single exponential function. Its time constant corresponds to the product of the series resistance and the total membrane capacity. In addition, the capacitive currents in the voltage clamp regime simulated after the addition of a series resistance of $R_s = 2 M\Omega$ into the scheme in Fig. 2 did not depend appreciably on the incorporation of the TATS (not shown).

As follows from this reasoning, the final velocity of electrical signal propagation in the TATS can hardly have a significant effect on the whole-cell electrical activity. However, the effect due to the limited velocity of ionic diffusion in the tubules deserves consideration. As shown in Fig. 4, significant variations in the ionic concentration of calcium and potassium become apparent in the tubules under normal steady state conditions.

It is remarkable that the largest change in tubular ionic concentrations was the depletion of Ca^{2+} ions by almost 13%, whereas K^+ accumulation was less than 5%. Both of these effects had been evaluated (K^+ accumulation: Attwell et al. 1979; Ca^{2+} depletion: Bers 1983) but were attributed to narrow intercellular spaces (i.e. clefts). The present modelling clearly shows that these properties are readily borne by each cardiac ventricular cell, owing to the presence of the TATS and to the preferential localization of Ca^{2+} and K^+ channels to its membrane.

These changes, though not dramatic, are likely to affect the conditions for the appearance of afterdepolarizations and triggered arrhythmias. In particular, tubular Ca^{2+} depletion lowers Ca^{2+} entry through I_{CaL} channels and consequently may retard or limit arrhythmogenesis in conditions of intracellular Ca^{2+} overload. The functional outcome of tubular K^+ accumulation is more difficult to analyse, since an increase of $[\text{K}^+]_t$ increases the conductance of tubular K^+ channels following approximately the square root of $[\text{K}^+]_t$, which would stabilize the resting membrane voltage. At the same time, however, the equilibrium voltage for K^+ ions is shifted positively, bringing the membrane resting voltage nearer to the threshold for triggered activity. Estimating whether one or the other effect shall dominate in a given situation is ideally suited to the present quantitative modelling approach. These important issues will be addressed in separate work.

Simulated voltage clamp experiments demonstrated that the variations in tubular ionic concentrations could transpire under certain experimental conditions as modulation of the recorded membrane currents. In the example illustrated in Fig. 5, potassium currents were large enough to produce prominent changes of $[\text{K}^+]_t$. According to the model, the depletion of K^+ in the TATS led to a slow decline of I_{K1} due to a decrease of both the conductance g_{K1} and the driving force $V_m - V_K$. Similar responses of the inward rectifying K^+ current to hyperpolarizing steps were observed in cat ventricular myocytes by Harvey and Ten Eick (1988) who attributed it partly to a voltage-dependent inactivation and partly to a drop of $[\text{K}^+]$ from 5.6 mmol/l to 3.75 mmol/l in 70 ms at -170 mV in an unidentified extracellular compartment. Our quantitative modelling (Fig. 5) is in agreement with this measurement and shows that most of the I_{K1} decay during hyperpolarization can be accounted for by tubular K^+ depletion.

When simulating another kind of voltage-clamp experiments, the present model was not able to reproduce the slowly decaying inward 'tail currents' following depolarizing impulses as observed in mouse ventricular myocytes (Clark et al. 2001). The authors interpreted the tail currents as a decline of I_{K1} caused by decaying accumulation of K^+ in the TATS. The reason for this difference is that in our model the depolarization-induced potassium currents are not large enough to induce a prominent accumulation of ions, comparable to that occurring in mouse or rat ventricular cells. Indeed, Clark et al. (2001) did not observe these tail currents in atrial myocytes where the TATS is poorly developed. In return, if the 'rat-like' potassium currents were inserted into the present model (not shown), the slowly decaying inward tail currents that followed depolarizing but not hyperpolarizing pulses appeared.

In conclusion, the present model helps to interpret the experimental data relating to the cardiac TATS. It is a valuable tool to investigate the functional role of this structure in physiological and pathological states of the ventricular myocytes and to suggest new experimental investigations.

Acknowledgements. This study was supported by the grant 204/02/D129 from the Grant Agency of the Czech Republic, by project AVOZ 2076919 from the Institute of Thermomechanics of Czech Academy of Sciences and by the project J07/98:141100004 from the Ministry of Education, Youth and Sports of the Czech Republic. The authors thank Dr. M. Šimurdová for reading the manuscript and comments.

References

- Amsellem J., Delorme R., Souchier C., Ojeda C. (1995): Transverse-axial tubular system in guinea pig ventricular cardiomyocyte: 3D reconstruction, quantification and its possible role in K^+ accumulation-depletion phenomenon in single cells. *Biol. Cell* **85**, 43–54
- Attwell D., Cohen I., Eisner D. (1979): Membrane potential and ion concentration stability conditions for a cell with restricted extracellular space. *Proc. R. Soc. London, Ser. B* **206**, 145–161
- Baumgarten C. M., Cohen C. J., McDonald T. F. (1981): Heterogeneity of intracellular potassium activity and membrane potential in hypoxic guinea pig ventricle. *Circ. Res.* **49**, 1181–1189
- Beeler G. W., Reuter H. (1977): Reconstruction of the action potential of ventricular myocardial fibres. *J. Physiol. (London)* **268**, 177–210
- Bers D. M. (1983): Early transient depletion of extracellular Ca during individual cardiac muscle contractions. *Am. J. Physiol.* **244**, H462–468
- Brown A. M., Lee K. S., Powell T. (1981): Sodium current in single rat heart muscle cells. *J. Physiol. (London)* **318**, 479–500
- Chen F., Mottino G., Klitzner T. S., Philipson K. D., Frank J. S. (1995): Distribution of the Na^+/Ca^{2+} exchange protein in developing rabbit myocytes. *Am. J. Physiol.* **268**, C1126–1132
- Christé G. (1999): Localization of K^+ channels in the T-tubules of cardiomyocytes as suggested by the parallel decay of membrane capacitance, IK_1 , and IK_{ATP} during culture and by delayed IK_1 response to barium. *J. Mol. Cell. Cardiol.* **31**, 2207–2213
- Clark R. B., Tremblay A., Melnyk P., Allen B. G., Giles W. R., Fiset C. (2001): T-tubule localization of the inward-rectifier K^+ channel in mouse ventricular myocytes: a role in K^+ accumulation. *J. Physiol. (London)* **537**, 979–992
- Daut J. (1982): The passive electrical properties of guinea-pig ventricular muscle as examined with a voltage-clamp technique. *J. Physiol. (London)* **330**, 221–242
- DiFrancesco D., Noble D. (1985): A model of cardiac electrical activity incorporating ionic pumps and concentration changes. *Philos. Trans. R. Soc. London, Ser. B* **307**, 353–398
- Doyle D. D., Kamp T. J., Palfrey H. C., Miller R. J., Page E. (1986): Separation of cardiac plasmalemma into cell surface and T-tubular components. Distribution of saxitoxin- and nitrendipine-binding sites. *J. Biol. Chem.* **261**, 6556–6563
- Faber G. M., Rudy Y. (2000): Action potential and contractility changes in $[Na^+]_i$ overloaded cardiac myocytes: a simulation study. *Biophys. J.* **78**, 2392–2404

- Frank J. S., Mottino G., Reid D., Molday R. S., Philipson K. D. (1992): Distribution of the Na^+ - Ca^{2+} exchange protein in mammalian cardiac myocytes: an immunofluorescence and immunocolloidal gold-labeling study. *J. Cell. Biol.* **117**, 337—345
- Harrison S. M., McCall E., Boyett M. R. (1992): The relationship between contraction and intracellular sodium in rat and guinea-pig ventricular myocytes. *J. Physiol. (London)* **449**, 517—550
- Harvey R. D., Ten Eick R. E. (1988): Characterization of the inward-rectifying potassium current in cat ventricular myocytes. *J. Gen. Physiol.* **91**, 593—615
- Hilgemann D. W., Noble D. (1987): Excitation-contraction coupling and extracellular calcium transients in rabbit atrium: reconstruction of basic cellular mechanisms. *Proc. R. Soc. London, Ser. B* **230**, 163—205
- Hodgkin A. L., Huxley A. F. (1952): A quantitative description of membrane current and its application to conduction and excitation in nerve. *J. Physiol. (London)* **117**, 500—544
- Hund J. H., Kucera J. P., Otani N. F., Rudy Y. (2001): Ionic charge conservation and long-term steady state in the Luo-Rudy dynamic cell model. *Biophys. J.* **81**, 3324—3331
- Iwata Y., Hanada H., Takahashi M., Shigekawa M. (1994): Ca^{2+} -ATPase distributes differently in cardiac sarcolemma than dihydropyridine receptor alpha 1 subunit and Na^+ / Ca^{2+} exchanger. *FEBS Lett.* **355**, 65—68
- Jafri M. S., Rice J. J., Winslow R. L. (1998): Cardiac Ca^{2+} dynamics: The roles of ryanodine receptor adaptation and sarcoplasmic reticulum load. *Biophys. J.* **74**, 1149—1168
- Luo C., Rudy Y. (1991): A model of the ventricular cardiac action potential. Depolarization, repolarization, and their interaction. *Circ. Res.* **68**, 1501—1526
- Luo C. H., Rudy Y. (1994): A dynamic model of the cardiac ventricular action potential. I. Simulations of ionic currents and concentration changes. *Circ. Res.* **74**, 1071—1096
- Mays D. J., Foose J. M., Philipson L. H., Tamkun M. M. (1995): Localization of the $\text{Kv}1.5$ K^+ channel protein in explanted cardiac tissue. *J. Clin. Invest.* **96**, 282—292
- McAllister R. E., Noble D., Tsien R. W. (1975): Reconstruction of the electrical activity of cardiac Purkinje fibres. *J. Physiol. (London)* **251**, 1—59
- McDonough A. A., Zhang Y., Shin V., Frank J. S. (1996): Subcellular distribution of sodium pump isoform subunits in mammalian cardiac myocytes. *Am. J. Physiol.* **270**, C1221—1227
- Noble D. (1962): A modification of the Hodgkin-Huxley equations applicable to Purkinje fibre action and pacemaker potential. *J. Physiol. (London)* **160**, 317—352
- Nordin C. (1993): Computer model of membrane current and intracellular Ca^{2+} flux in the isolated guinea pig ventricular myocyte. *Am. J. Physiol.* **265**, H2117—2136
- Nygren A., Fiset C., Firek L., Clark J. W., Lindblat D. S., Clark R. B., Giles W. R. (1998): Mathematical model of an adult human atrial cell. The role of K^+ currents in repolarization. *Circ. Res.* **82**, 63—81
- Petrecca K., Amellal F., Laird D. W., Cohen S. A., Shrier A. (1997): Sodium channel distribution within the rabbit atrioventricular node as analysed by confocal microscopy. *J. Physiol. (London)* **501**, 263—274
- Shepherd N., McDonough H. B. (1998): Ionic diffusion in transverse tubules of cardiac ventricular myocytes. *Am. J. Physiol.* **275**, H852—860
- Siri F. M., Krueger J., Nordin C., Ming Z., Aronson R. S. (1991): Depressed intracellular calcium transients and contraction in myocytes from hypertrophied and failing guinea pig hearts. *Am. J. Physiol.* **261**, H514—530

- Soeller C., Cannell M. B. (1999): Examination of the transverse tubular system in living cardiac rat myocytes by 2-photon microscopy and digital image-processing techniques. *Circ. Res.* **84**, 266—275
- Sun X. H., Protasi F., Takahashi M., Takeshima H., Ferguson D. G., Franzini-Armstrong C. (1995): Molecular architecture of membranes involved in excitation-contraction coupling of cardiac muscle. *J. Cell. Biol.* **129**, 659—671
- Šimurda J., Šimurdová M., Čupera P. (1988): 4-Aminopyridine sensitive transient outward current in dog ventricular fibres. *Pflügers Arch.* **411**, 442—449
- Takeuchi S., Takagishi Y., Yasui K., Murata Y., Toyama J., Kodama I. (2000): Voltage-gated K^+ Channel, Kv4.2, localizes predominantly to the transverse-axial tubular system of the rat myocytes. *J. Mol. Cell. Cardiol.* **32**, 1361—1369
- Tseng G. N., Hoffman B. F. (1989): Two components of transient outward current in canine ventricular myocytes. *Circ. Res.* **64**, 633—647
- Yao A., Spitzer K. W., Ito N., Zaniboni M., Lorell B. H., Barry W. H. (1997): The restriction of diffusion of cations at the external surface of cardiac myocytes varies between species. *Cell Calcium* **22**, 431—438
- Yasui K., Anno T., Kamiya K., Boyett M. R., Kodama I., Toyama J. (1993): Contribution of potassium accumulation in narrow extracellular spaces to the genesis of nicorandil-induced large inward tail current in guinea-pig ventricular cells. *Pflügers Arch.* **22**, 371—379
- Zahradník I., Pavelková J., Zahradníková A. (1996): Kinetic analysis of the calcium currents recorded from isolated cardiomyocytes. In: *Analysis of Biomedical Signals and Images* (Eds. J. Jan, P. Kilián, and I. Provazník), pp. 252—254, Technical University Press, Brno, Czech Republic

Final version accepted: April 4, 2003